

# A Solid-State Nuclear Magnetic Resonance Study of Post-Plasma Reactions in Organosilicone Microwave Plasma-Enhanced Chemical Vapor Deposition (PECVD) Coatings

Colin J. Hall,<sup>\*,†</sup> Thirunavukkarasu Ponnusamy,<sup>†</sup> Peter J. Murphy,<sup>‡</sup> Mats Lindberg,<sup>§</sup> Oleg N. Antzutkin,<sup>§,⊥</sup> and Hans J. Griesser<sup>‡</sup>

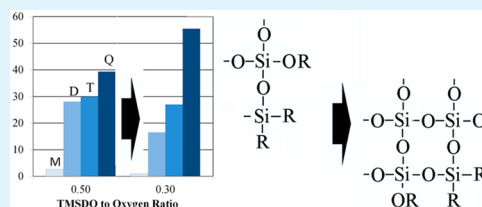
<sup>†</sup>Ian Wark Research Institute, University of South Australia, Mawson Lakes 5095, South Australia, Australia

<sup>‡</sup>Mawson Institute, University of South Australia, Mawson Lakes 5095, South Australia, Australia

<sup>§</sup>Chemistry of Interfaces, Luleå University of Technology, SE-97187, Luleå, Sweden

<sup>⊥</sup>Department of Physics, University of Warwick, Coventry CV4 7AL, United Kingdom

**ABSTRACT:** Plasma-polymerized organosilicone coatings can be used to impart abrasion resistance and barrier properties to plastic substrates such as polycarbonate. Coating rates suitable for industrial-scale deposition, up to 100 nm/s, can be achieved through the use of microwave plasma-enhanced chemical vapor deposition (PECVD), with optimal process vapors such as tetramethyldisiloxane (TMDSO) and oxygen. However, it has been found that under certain deposition conditions, such coatings are subject to post-plasma changes; crazing or cracking can occur anytime from days to months after deposition. To understand the cause of the crazing and its dependence on processing plasma parameters, the effects of post-plasma reactions on the chemical bonding structure of coatings deposited with varying TMDSO-to-O<sub>2</sub> ratios was studied with <sup>29</sup>Si and <sup>13</sup>C solid-state magic angle spinning nuclear magnetic resonance (MAS NMR) using both single-pulse and cross-polarization techniques. The coatings showed complex chemical compositions significantly altered from the parent monomer. <sup>29</sup>Si MAS NMR spectra revealed four main groups of resonance lines, which correspond to four siloxane moieties (i.e., mono (M), di (D), tri (T), and quaternary (Q)) and how they are bound to oxygen. Quantitative measurements showed that the ratio of TMDSO to oxygen could shift the chemical structure of the coating from 39% to 55% in Q-type bonds and from 28% to 16% for D-type bonds. Post-plasma reactions were found to produce changes in relative intensities of <sup>29</sup>Si resonance lines. The NMR data were complemented by Fourier transform infrared (FTIR) spectroscopy. Together, these techniques have shown that the bonding environment of Si is drastically altered by varying the TMDSO-to-O<sub>2</sub> ratio during PECVD, and that post-plasma reactions increase the cross-link density of the silicon–oxygen network. It appears that Si–H and Si–OH chemical groups are the most susceptible to post-plasma reactions. Coatings produced at a low TMDSO-to-oxygen ratio had little to no singly substituted moieties, displayed a highly cross-linked structure, and showed less post-plasma reactions. However, these chemically more stable coatings are less compatible mechanically with plastic substrates, because of their high stiffness.



**KEYWORDS:** NMR, organosilicone, graded, thin-films, plasma enhanced chemical vapor deposition (PECVD), postplasma

## I. INTRODUCTION

Transparent plastics, such as polycarbonate and poly(methyl methacrylate), are used widely in the automotive, aerospace, and ophthalmic industries. To ensure a long product life, these plastics must be protected via barrier coatings,<sup>1,2</sup> which must resist scratching and crazing.<sup>3,4</sup> One potential method of producing a barrier coating is with plasma-enhanced chemical vapor deposition (PECVD) using a silicon based precursor.

Early work used silane precursors,<sup>5,6</sup> but these are hazardous and require special handling. Siloxane process vapors have proven to be more user-friendly; for example, hexamethyldisiloxane (HMDSO), octamethyltrisiloxane (OMTS), octamethylcyclotetrasiloxane (OMCTS or OMCATS), vinyltetramethyldisiloxane (VTMDS), and tetramethyldisiloxane (TMDSO) have been studied.<sup>7–13</sup> TMDSO is a suitable candidate for industrial applications, because it has a high plasma deposition

rate and is relatively inexpensive.<sup>14,15</sup> In this study, a microwave PECVD system and mixed vapors of TMDSO and oxygen were used to deposit an amorphous organosilicone coating. The coating is graded in composition vertically by changing the TMDSO-to-oxygen ratio during deposition. At a high TMDSO-to-oxygen ratio, it is tailored to be more organic in nature at the interface with the polymeric substrate, and at a low TMDSO-to-oxygen ratio, it is more inorganic at the outer surface. The “softer”, organic–polymeric composition near the substrate interface provides better mechanical compliance with the substrate, thus reducing interfacial delamination stress,

**Received:** February 28, 2014

**Accepted:** May 2, 2014

**Published:** May 2, 2014

while the hard, glasslike outer layer provides excellent abrasion resistance.<sup>16,17</sup>

In developing such protective layers, we found that organosilicone coatings changed their characteristics over hours, days, and even months. Physically, they were observed to harden over time periods in the order of weeks, and, in some cases, they exhibited crazing when stored for time periods of weeks to months. The appearance of crazing poses a significant limitation in the practical application of this coating technology.

We hypothesized that the observed crazing results from mechanical stresses induced into the coating by post-plasma chemical reactions that are likely to be oxidative in nature, in analogy to documented oxidative reaction cycles that occur in other plasma polymers as atmospheric oxygen diffuses into the coating and reacts with the remaining trapped radicals.<sup>18–22</sup> Previous studies with similar organosiloxane monomers (HMDSO, OMCTS, DVTMDSO)<sup>5,18–21</sup> have reported such post-plasma reactions. Specifically, Wrobel<sup>5</sup> studied radio-frequency (rf) PECVD of HMDSO using attenuated total reflectance–Fourier transform infrared spectroscopy (ATR-FTIR) and reported changes in the bonding between –OH, >C=O, Si–O–Si, and Si–O–C groups with a decay of Si–H bands in the spectra. Wrobel et al.<sup>23</sup> also noted that the complex plasma process leads to complex siloxane chemistry. Hegemann et al.<sup>20</sup> showed stable surface energy of HMDSO coatings deposited above the activation energy of the system, which is related to the ratio of applied power per unit monomer flow. Gengenbach and Griesser,<sup>19</sup> on the other hand, found only minor changes in surface energy and chemistry of rf-deposited HMDSO coatings. The aforementioned studies used rf excitation frequency in reactors of differing geometries. The complex nature of the plasma process, along with system-dependent coating properties, make generalization difficult.

There is limited information on the aging process for PECVD coatings made from TMDSO and less so for systems using microwave frequencies. Muir et al.,<sup>24</sup> using a similar deposition system as in this study, described adhesion loss during aging, and they postulated on the uptake of oxygen and ensuing oxidative radical reactions at the interface as the mechanism behind the change in adhesion with time. Changes to other properties with time were not described.

In this study, solid-state nuclear magnetic resonance (solid-state NMR) and Fourier transform infrared (FTIR) spectroscopy were used to identify the post-plasma reactions occurring in the organosilicone coatings. Changes in coating chemistry may lead to changes in intrinsic stress and, as such, will affect the stress balance and may lead to coating failure by either stress crazing or delamination.

This study reports on the use of single-pulse excitation (SPE) <sup>29</sup>Si magic-angle-spinning (MAS) NMR, henceforth referred to as quantitative NMR, with three coatings made with different TMDSO-to-oxygen ratios, to obtain quantitative data on the Si–O (siloxane) network within the coatings. The TMDSO-to-oxygen ratios chosen are from the monomer-rich region, transition region, and the monomer-deficient region of the plasma process. These reaction zones have been reported elsewhere for similar systems.<sup>21,25</sup> These ratios are representative of the ratios used in the development of the graded coatings. The ratio of TMDSO-to-oxygen flows has been reported by Goujon et al.<sup>26</sup> and Bapin and von Rohr<sup>27</sup> as a powerful way to vary coating chemistry. In the organosilicon coatings, the primary nuclei of NMR interest are <sup>1</sup>H, <sup>13</sup>C, and <sup>29</sup>Si. Through the use of MAS, the broadening of NMR

resonance lines due to anisotropic interactions, such as the chemical shift anisotropy and the dipole–dipole interactions in polycrystalline or glasslike solid samples, can be overcome. MAS at moderate spinning frequencies, 5–10 kHz, averages out second-rank tensorial interactions for spin-1/2 nuclei, such as <sup>13</sup>C and <sup>29</sup>Si. However, very high spinning MAS (≥100 kHz) is needed to average out <sup>1</sup>H–<sup>1</sup>H homonuclear dipole–dipole interactions in solids and to achieve a reasonably high resolution in <sup>1</sup>H MAS NMR spectra. Therefore, the complex bonding structure of siloxane molecules in plasma polymers can be readily elucidated using <sup>13</sup>C and <sup>29</sup>Si MAS NMR, while special high-spinning MAS probes will be needed for high-resolution <sup>1</sup>H MAS NMR spectroscopy of these systems.

<sup>29</sup>Si and <sup>13</sup>C cross-polarization (CP) MAS NMR (henceforth referred to as qualitative NMR) was also used to study the post-plasma reactions over 2 months. CP from <sup>1</sup>H to <sup>29</sup>Si nuclei enhances the signal from the <sup>29</sup>Si sites, which are coupled to nearby <sup>1</sup>H nuclei through the heteronuclear <sup>1</sup>H–<sup>29</sup>Si dipole–dipole interaction. Therefore, the <sup>29</sup>Si NMR signal is semi-quantitative, since intensities of resonance lines depend on many experimental parameters, such as the number of nearby protons, CP contact time (ct), and the relaxation time of the CP signal in the rotating frame (i.e., during ct) (*T*<sub>1ρ</sub>). However, the experimental time is considerably shorter for the CP measurements, because of a considerably shorter spin–lattice relaxation time of protons, *T*<sub>1</sub>(<sup>1</sup>H), compared to *T*<sub>1</sub>(<sup>13</sup>C) and *T*<sub>1</sub>(<sup>29</sup>Si) that allows for relatively small changes in NMR spectra to be observed with a higher confidence.

<sup>29</sup>Si and <sup>13</sup>C MAS NMR are powerful tools for the investigation of the chemical bonding environments (functionality) of these elements within a PECVD coating, given the complex chemistry involved in the deposition process.<sup>28</sup> The plasma can form radicals, excited molecules, energetic photons, and neutral molecules, and this abundance of species can lead to a complex chemistry and a heterogeneous deposition. Conventional nomenclature for the four possible oxygen-binding states of Si in siloxanes is M (monofunctional), D (difunctional), T (trifunctional), and Q (quaternary), which relates to the number of O atoms bonded to a Si atom. The chemical shift range due to these bond configurations spreads from +10 ppm to –110 ppm. In addition, shifts due to substitution of nearest-neighbor atoms can be observed and can be used to fully resolve the structure of siloxanes. It has been used to determine silicon oil structure, in biology to determine diatom structure,<sup>29</sup> and to determine the structure of some plasma polymers.<sup>30–33</sup>

However, the application of NMR to PECVD coatings has been limited; this is due mainly to the sample requirements for the measurement. Solid-state NMR of magnetic nuclei with a low natural abundance (4.7% n.a. for <sup>29</sup>Si and 1.08% n.a. for <sup>13</sup>C) requires at least a few tens of milligrams of a powdered sample. Most PECVD systems cannot produce this amount under normal operating conditions, and attempts to collect enough sample material would require very long deposition times, which could change the coating chemistry.<sup>33,34</sup> With our microwave PECVD system, the deposition rates are fast enough to collect a sufficient quantity without any modification and over normal deposition times.

In addition, FTIR measurements were simplified as the thick coatings (4 μm) deposited under normal conditions were easily measurable in transmission mode with a sufficient signal-to-noise ratio.

## II. EXPERIMENTAL SECTION

**A. Deposition Conditions and Sample Preparation.** The deposition was done in a custom-built reactor, shown in Figure 1. The

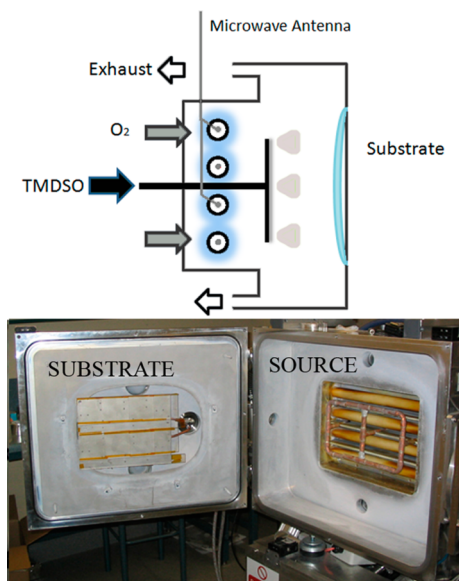


**Figure 1.** Schematic diagram and photograph of the deposition system.

design is based on systems developed by both Leybold GmbH<sup>35</sup> and Muegge GmbH.<sup>36</sup> The main chamber, which held the substrates, had a volume of  $\sim 62\,500\text{ cm}^3$  (62.5 L). Microwave power at 2.45 GHz and up to 6 kW (GMP 60K S/D, Sairem, Lyon, France) was fed through a rectangular waveguide, which consisted of a three-stub “autotuner” and sliding short. This maintained reflected power to below 10% of the forward power. A cone antenna fed the microwave power to a coaxial waveguide system which further split the microwave power into both ends of four copper antennas (outer diameter of OD = 6 mm). The antennas were fed down the center of four aluminum oxide tubes (OD = 25.4 mm). The tubes were located along one wall of the chamber and were semienclosed by aluminum walls to form the plasma zone, with high-purity oxygen fed directly into this region. The total volume of the plasma glow was  $\sim 9700\text{ cm}^3$ , which was much larger than in most previous studies and required the plasma power levels used in this study to produce uniform glow zones. The precursor vapor (tetramethyldisiloxane (TMDSO), Sigma–Aldrich, Australia) was used to enable deposition. The precursor was fed separately through a gas manifold aimed directly at the substrates, which were located facing the tubes. The manifold consisted of three individual pieces: two rectangular ends and a center H piece with multiple small holes. These pieces could be translated toward the substrate or the holes selectively blocked, to optimize coating uniformity. A  $\sim 120\text{ mm}$  distance between monomer ring and substrate was used. Monomer and gas flows were regulated via mass flow controllers (MFCs) (Low- $\Delta P$ -Flow, Bronkhorst High-Tech BV, The Netherlands, and Unit Instruments, Model UFC-8100, USA, respectively). The chamber was evacuated with a Roots blower (605  $\text{m}^3/\text{h}$ , Edwards, Model EH500) and rotary pump (80  $\text{m}^3/\text{h}$ , Edwards, Model E2M80) combination. The chamber pressure was monitored with a capacitance manometer (MKS, Model 628), and the system was controlled via a programmable logic controller (PLC).

Coatings for the quantitative NMR experiments were performed at constant TMDSO flow of 150 sccm with  $\text{O}_2$  flow at 300, 400, and 500 sccm. This corresponded to a TMDSO-to-oxygen ratio of 0.5, 0.375 and 0.3, respectively. Chamber pressure was between 50 and 70 Pa. Coatings for qualitative (CP/MAS) NMR experiments were deposited with TMDSO-to-oxygen ratios of 0.3, 0.18, and 0.05. TMDSO/ $\text{O}_2$

flows used were  $\sim 75/250$ ,  $52/280$ , and  $15/315$  sccm. Chamber pressure was between 35 Pa and 38 Pa.

Stainless-steel pieces  $100\text{ mm} \times 150\text{ mm}$  were used as collection plates for MAS NMR sample preparation. Flakes of the coatings were shaved off the stainless-steel plates with a razor blade. Deposition to a thickness of  $\sim 3\text{ }\mu\text{m}$  was repeated three times, each deposition generated  $\sim 90\text{ mg}$ . Approximately 250 mg was collected for each condition and packed into zirconia NMR rotors with diameters of 4 mm (for CP/MAS NMR) and 7.5 mm (for SPE/MAS NMR). For FTIR, potassium bromide (KBr) was pressed into pellets and dried in an oven before coating under the same plasma conditions. Coatings of thickness  $\sim 4\text{ }\mu\text{m}$  were deposited onto the dried KBr pellets. Coating thickness was determined by a spectral reflectometer (Model F20, Filmetrics, San Diego, CA). All samples were stored under ambient conditions ( $20 \pm 2\text{ }^\circ\text{C}$ , relative humidity of RH = 40%–60%) in Petri dishes (to avoid contamination) and tested regularly over a period of eight weeks.

**B. Characterization Methods.** Solid-state single-pulse-excitation (SPE)  $^{29}\text{Si}$  MAS NMR spectra were recorded on an Agilent/Varian/Chemagnetics Model Infinity CMX-360 spectrometer using a single-pulse experiment with phase-modulated (TPPM) proton decoupling with the nutation frequency of protons equal to 40.6 kHz. The  $^{29}\text{Si}$  operating frequency was 71.5098 MHz. The  $90^\circ$  and  $180^\circ$  pulse durations were 8.5 and 17.0  $\mu\text{s}$ , respectively. Spin–lattice relaxation time,  $T_1(^{29}\text{Si})$ , of organosilicone coatings was found to be 50–55 s, as measured using the standard inversion recovery experiment:  $180^\circ$ -tau- $90^\circ$ -acq. Therefore, the recycling time (pulse delay, pd) in SPE experiments was chosen to be 275 s, to avoid signal saturation and ensure quantitative NMR measurements, i.e.,  $\text{pd} \geq 5T_1(^{29}\text{Si})$ . To achieve a reasonably high signal-to-noise ratio ( $S/N > 10$ ) in NMR spectra, from 280 to 316, signal transients were accumulated for different samples of organosilicone coatings that corresponded to the total experimental time for one SPE  $^{29}\text{Si}$  MAS NMR measurement of ca. 21.4–24.1 h. Samples of organosilicone coatings (ca. 250 mg) were packed into zirconium dioxide standard double bearing 7.5 mm rotors. The spinning frequency for all samples was 4500 Hz, and it was stabilized to  $\pm 1\text{ Hz}$  using an internal stabilization device. All  $^{29}\text{Si}$  chemical shift data were externally referenced to a liquid sample of tetramethylsilane (TMS, 0 ppm) in a 4-mm glass tube placed in a 7.5 mm rotor to minimize differences in magnetic susceptibility between rotors with coatings and the external reference sample. All solid-state  $^{29}\text{Si}$  MAS NMR spectra were recorded at ambient temperature (ca. 293 K). NMR analysis of coatings was performed approximately 6–8 weeks after sample preparation.

Semiquantitative solid-state  $^{29}\text{Si}$  and  $^{13}\text{C}$  CP/MAS NMR measurements with proton decoupling were performed using a Bruker Model Avance II 300 MHz ultrashield NMR spectrometer at a frequency of 59.6 and 75.4 MHz for  $^{29}\text{Si}$  and  $^{13}\text{C}$  nuclei, respectively. CP contact time was 2 ms for both  $^1\text{H}$ - $^{29}\text{Si}$  and  $^1\text{H}$ - $^{13}\text{C}$  CP/MAS NMR experiments. A sample with liquid TMS was used as the external reference. MAS and a recycling delay were 10 kHz and 5 s, respectively. An in-built software, “Topspin 2.0”, was used for the processing and analysis of obtained NMR spectra. Spectra were recorded 24 h after deposition and then at regular intervals for 8 weeks.

FTIR spectra were obtained in transmission mode using a Nicolet Model Magna-IR 750 with nitrogen purge.

## III. RESULTS

**A. Film Structure. 1. Quantitative Single Pulse Excitation  $^{29}\text{Si}$  MAS NMR.** Single-pulse excitation  $^{29}\text{Si}$  MAS NMR spectra of the coatings deposited at TMDSO-to- $\text{O}_2$  ratios of 0.5, 0.375, and 0.3 are shown in Figure 2. As previously indicated, these ratios are indicative of the process conditions used in the development of the graded coating. The monomer, TMDSO, is known to give rise to a single resonance line at approximately  $-5\text{ ppm}$  ( $M^{\text{H}}$ ).<sup>37</sup> In contrast, the resonances lines assigned to different  $^{29}\text{Si}$  sites in the organosilicone coating extend from

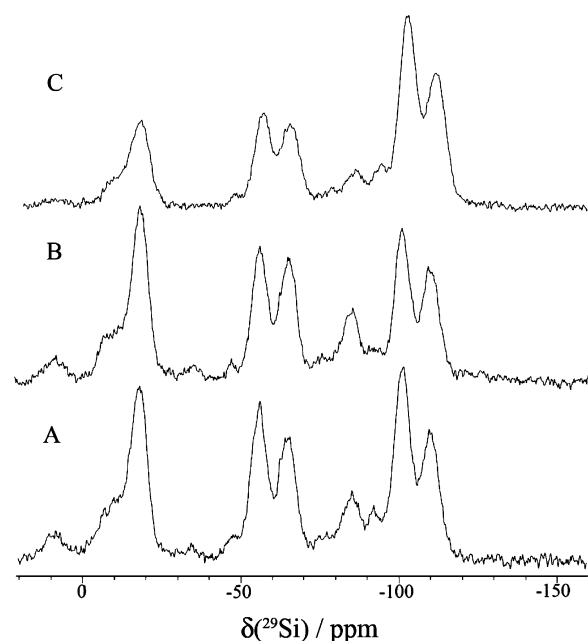


**Figure 2.** SPE  $^{29}\text{Si}$  MAS NMR spectra of coatings deposited with TMDSO-to-oxygen ratios of 0.5 (spectrum A), 0.375 (spectrum B), and 0.3 (spectrum C). The MAS frequency was 4.5 kHz. Spectra are offset for clarity.

+10 ppm to  $-110$  ppm. Figure 2 shows that there are 12 clearly distinguishable resonances positioned at isotropic chemical shifts,  $\delta(^{29}\text{Si})$  (see Table 1). The number of resonances suggests a high level of molecular fragmentation and rearrangement due to the plasma deposition process performed at different TMDSO/ $\text{O}_2$  ratios. The mechanism behind PECVD has been explored by Alexander et al.,<sup>38</sup> Rau and Kulisch,<sup>18</sup> and Tajima and Yamamoto.<sup>39</sup> The complex chemistry involves free radicals, molecular fragments, electrons, ions, and photons. Because of the fragmentation effect of the high frequency and high energy of the microwave plasma, there is no significant limitation on the bonds that can be formed, in contrast to traditional polymerization, and, hence, Si atoms are observed in a wide range of bonding environments. The spectra consist of many resonance lines corresponding to M-, D-, T-, and Q-type

bonding environments, where Si has bonded to one, two, three, or four O atoms, respectively. Subresonance signals are assigned to  $^{29}\text{Si}$  sites with nearest neighbors, i.e., H,  $\text{CH}_2$ ,  $\text{CH}_3$ , OH, or  $\text{OCH}_3$ , as will be analyzed and specifically discussed in detail below. The many upfield shifts observed suggest extensive cross-linking or substitution of some of the methyl groups by hydrogen and hydroxyl groups. The high resolution obtained has been achieved through the collection of a significant volume of sample, and the clearly defined resonances allow improved assignments and give a clear trend when investigating post-plasma reactions, as will be discussed later.

SPE  $^{29}\text{Si}$  MAS NMR spectra for the coatings deposited at ratios of 0.5 and 0.375 are very similar. A difference is observed for the coatings deposited at a ratio of 0.3, i.e., at a higher relative amount of oxygen during plasma polymerization. A decrease in the M-, D-, and T-bond bonding environments is observed with a concurrent increase in the Q-type bonding environments. These spectra were subsequently analyzed and used to determine the percentage of bonding environments for  $^{29}\text{Si}$  and this is presented in Table 1 and Figures 3 and 4.

The quantitative NMR data for the individual M-, D-, T-, and Q-type Si nuclei were normalized to the total Si content (total integral intensity of all resonance lines in corresponding SPE  $^{29}\text{Si}$  MAS NMR spectra), as shown in Figure 3. The 0.5 and 0.375 ratio coatings show a reduced level of Q-type bonding and concurrent increase in M-, D-, and T-type bonding (left and middle panels in Figure 3). For the 0.3 flow ratio coating,  $\sim 55\%$  of the Si atoms are in the Q-type coordination (i.e., bound to four O atoms).

The quantitative  $^{29}\text{Si}$  MAS NMR data were further analyzed to elucidate the extent of branching (Q4, Q3, and T3), the extent of linear structural elements (Q2, T2, and D2) and the extent of termination (Q1, T1, and M), as exemplified in Figure 4. The 0.5 and 0.375 ratio coatings show similar structural information, that is, branching  $\sim 45\%$ , linear chains  $\sim 43\%$  and terminations at  $\sim 10\%$ . This is most likely a result of the plasma chemistry reaching a level of TMDSO saturation, as will be discussed below. The 0.3 ratio coating is predominantly composed of siloxane in the form of branching (62%) and linear chains (30%) with only a small number of terminations ( $\sim 7\%$ ). This can be interpreted as follows, as the TMDSO-to-

**Table 1.** Assignments for SPE  $^{29}\text{Si}$  MAS NMR Spectra of Coatings Prepared with Different TMDSO/ $\text{O}_2$  Ratios

	TMDSO-to-oxygen ratio = 0.5		TMDSO-to-oxygen ratio = 0.375		TMDSO-to-oxygen ratio = 0.3	
	$\delta(^{29}\text{Si})$ / ppm	integral intensity	$\delta(^{29}\text{Si})$ / ppm	integral intensity	$\delta(^{29}\text{Si})$ / ppm	integral intensity
Q4 - $\text{Si}(\text{OSi})_4$	-109.9	137.9	-109.7	126.7	-110.1	223.4
Q3 - $\text{Si}(\text{OSi})_3\text{OH}$	-100.9	164.3	-100.7	200.6	-101.0	288.2
Q2 - $\text{Si}(\text{OSi})_2(\text{OH})_2$	-92.3	15.5	-91.9	21.6	-92.2	29.8
Q1 - $\text{Si}(\text{OSi})(\text{OH})_3$	-84.7	88.5	-84.6	69.8	-84.3	52.6
T3(H) - $\text{Si}(\text{OSi})_3\text{H}$	-76.1	14	-76.2	10.6	-77.1	17.3
T3 - $\text{Si}(\text{OSi})_3\text{C}$	-65.0	144.6	-64.5	127.1	-63.9	139.9
T2 - $\text{Si}(\text{OSi})_2(\text{OH})\text{H}$	-55.9	146.9	-55.4	151.5	-55.3	121.1
T1 - $\text{Si}(\text{OSi})(\text{OH})_2\text{C}$	-46.9	4	-46.9	7	-46.7	11.4
D2(H) - $\text{Si}(\text{OSi})_2\text{CH}$	-35.0	8.8	-34.2	2.8		
D2 - $\text{Si}(\text{OSi})_2\text{C}_2$ , low mobility	-18.2	203.3	-17.7	167.7	-16.6	143.9
D2 - $\text{Si}(\text{OSi})_2\text{C}_2$ , mobile	-9.4	77.6	-9.7	93.5	-7.8	33.4
M - $\text{Me}_3\text{SiOSi}$	9.1	27.5	9.3	27.4	9.9	10.6

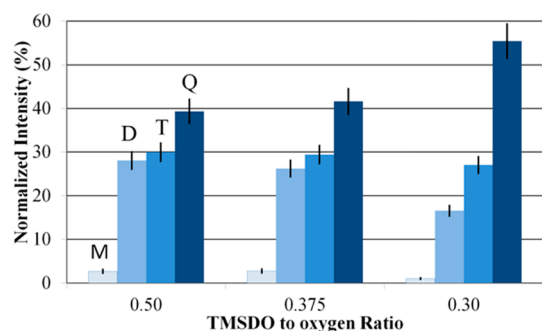


**Figure 3.** Normalized integral intensity of M-type (pale blue), D-type (light blue), T-type (medium blue), and Q-type (dark blue) signal components in SPE  $^{29}\text{Si}$  MAS NMR spectra of coatings prepared with different TMSDO/ $\text{O}_2$  ratios: 0.50 (left panel), 0.38 (middle panel), and 0.30 (right panel). The size of the error bars were determined from error analysis during the curve-fitting procedure.

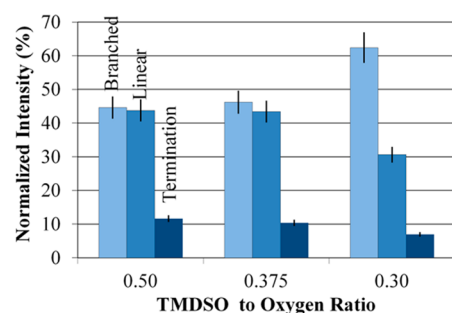


**Figure 4.** Normalized integral intensities of the various types of Si–O bonding: branching (light blue), linear (medium blue), and termination (dark blue) in SPE  $^{29}\text{Si}$  MAS NMR spectra of coatings prepared with different TMSDO/ $\text{O}_2$  ratios: 0.50 (left panel), 0.38 (middle panel), and 0.30 (right panel). The size of the error bars were determined from error analysis during the curve-fitting procedure.

oxygen ratio is decreased the extent of cross-linking increases (as shown by the large increase in the branching) and the extent of linear structural elements decreases.

2.  $\text{SPE } ^{13}\text{C MAS NMR}$ . Table 2 shows the interpretation of the  $^{13}\text{C}$  chemical shifts from SPE  $^{13}\text{C}$  MAS NMR spectra for the three coatings. Assignments of resonance lines were based on  $^{13}\text{C}$  chemical shifts reported previously.<sup>33,40</sup> The integral intensity has been qualitatively assigned as “very weak”, “weak”, “medium” and “strong”. Predominantly the  $^{13}\text{C}$  atoms are in the form of methyl groups, either in a termination arrangement

$(\text{CH}_3)_3-(\text{Si})-\text{O}-$  or in the linear chain  $(\text{CH}_3)_2-(\text{Si})-(\text{O})_2$ . Resonances of considerably lesser intensity are observed from methoxy, alcohols, alkenes, and carbonyl groups. These tend to disappear for the coating with a TMSDO-to-oxygen ratio of 0.3. This trend is consistent with that seen in the SPE  $^{29}\text{Si}$  MAS NMR spectra, in that the coatings become less organic and shift toward a largely inorganic siloxane-dominated structure at high oxygen admixture.

3. *Semiquantitative  $^{29}\text{Si}$  CP/MAS NMR*. Coatings deposited with TMSDO-to-oxygen ratios of 0.3, 0.18, and 0.05 were studied using semiquantitative  $^{29}\text{Si}$  CP/MAS NMR experiments. These ratios were chosen to represent depositions from the monomer-rich region, transition region, and monomer-deficient region, as defined by the deposition rate. The samples prepared for quantitative SPE  $^{29}\text{Si}$  MAS NMR measurements discussed above did not show a large variation in chemistry; thus, a different set of samples was chosen to span a larger chemistry range via a larger variation in the TMSDO-to-oxygen ratio, positioned on either side of a step change in process chemistry. Note that, because of the long spin–lattice relaxation times of  $^{29}\text{Si}$  sites in coatings, SPE  $^{29}\text{Si}$  MAS NMR experiments would require  $\sim 20\text{--}24$  h per sample; thus, NMR signals will be additionally affected by post-deposition chemical processes in coatings. In turn,  $^{29}\text{Si}$  CP/MAS NMR relies upon spin–lattice relaxation times of protons, which are usually much shorter in solids (from hundreds of milliseconds to a few seconds), and these NMR experiments would require experimental times of  $\sim 1$  h (or less) per sample. However, Si sites that are in closer spatial vicinity to protons will acquire a larger integral intensity during  $^1\text{H}-^{29}\text{Si}$  cross-polarization (thus, the CP/MAS NMR technique is “semi-quantitative”).

Figure 5 shows  $^{29}\text{Si}$  CP/MAS NMR spectra for coatings with TMSDO-to-oxygen ratios of 0.3, 0.18 and 0.05, all measured 24 h after deposition. It can be seen that there are extensive differences between these three NMR spectra. The ratio of TMSDO to oxygen in the plasma has a large influence on the chemical composition of the coatings. As the ratio is decreased, the peaks corresponding to the organic structural elements are reduced or disappear, and the bonding tends toward that of a highly cross-linked Si–O–Si network, which could be described as more “silica-like” or “glass-like”.

4. *FTIR*. Figure 6 shows FTIR spectra for the 0.3, 0.18, and 0.05 ratio coatings. The spectra are similar to those reported by Pryce-Lewis et al.,<sup>10</sup> Wu and Gleason,<sup>30</sup> and Mei-Li et al.,<sup>41</sup> and the following peak assignments have been made using these references. A broad peak centered around  $3400\text{ cm}^{-1}$  is typical

**Table 2.** Assignments for SPE  $^{13}\text{C}$  MAS NMR Spectra of Coatings Prepared with Different TMSDO-to- $\text{O}_2$  Ratios

assignment <sup>a</sup>	TMSDO-to-oxygen ratio = 0.5		TMSDO-to-oxygen ratio = 0.375		TMSDO-to-oxygen ratio = 0.3	
	$\delta(^{13}\text{C})$ / ppm	integral intensity <sup>b</sup>	$\delta(^{13}\text{C})$ / ppm	integral intensity	$\delta(^{13}\text{C})$ / ppm	integral intensity
$(\text{CH}_3)_3-(\text{Si})-\text{O}-$	−3.1	medium	−3.0	medium	−3.1	medium
$(\text{CH}_3)_2-(\text{Si})-(\text{O})_2$	0.9	strong	1.0	strong	0.7	strong
C−(−C)	17.5	weak	18.4	weak		
methoxy*	40.3	medium				
alcohol, ether*	45.0	medium	45.3	medium	44.7	very weak
alcohol, ether*	51.6	medium	51.7	medium	51.0	weak
acetal*	$\sim 100$	weak (sb)	$\sim 103$	very weak		
alkene*	127.4	medium	$\sim 128$	weak		
quaternary alkene*	146.3	weak				
carbonyl (acid or ester)	184.4	weak	$\sim 178$	medium		

<sup>a</sup>Asterisk (\*) denotes putative assignment. <sup>b</sup>sb = sideband.

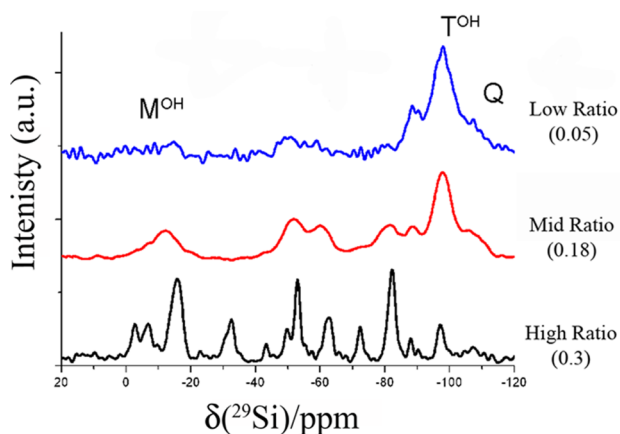


**Figure 5.**  $^{29}\text{Si}$  CP/MAS NMR spectra of coatings with TMDSO-to- $\text{O}_2$  ratios of 0.3 (bottom spectrum), 0.18 (middle spectrum), and 0.05 (top spectrum). Spectra have been offset for clarity.

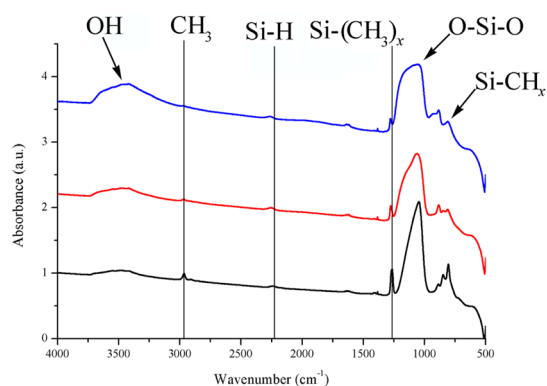


**Figure 6.** FTIR spectra for the 0.3 (bottom spectrum), 0.18 (middle spectrum), and 0.05 (top spectrum) ratio coatings. Spectra have been offset for clarity.

of the stretching vibration of  $-\text{OH}$ , most likely associated with  $\text{Si}-\text{OH}$ . This peak increases with decreasing TMDSO-to-oxygen ratio, and this agrees well with the solid-state NMR data, which show that the low ratio coating is dominated by  $\text{T}^{\text{OH}}$  groups. The asymmetric stretching mode of  $\text{CH}_2$  is observed at  $2939\text{ cm}^{-1}$ ; decreasing the feed gas ratio significantly reduces this peak, which is indicative of the more inorganic nature of the low ratio coatings. A peak at  $\sim 2200\text{ cm}^{-1}$  is assignable to  $\text{Si}-\text{H}$ ; this could be preserved from the parent monomer or as a result of fragmentation reactions. A sharp peak at  $1263\text{ cm}^{-1}$ , assignable to  $\text{Si}-(\text{CH}_3)_x$ , decreases as the ratio decreases; this is indicative of a coating with a reduced organic nature, via abstraction of methyl groups during deposition.<sup>5</sup> Linked with this are reduced intensities of the peaks at  $841$  and  $802\text{ cm}^{-1}$ , which can be assigned to the rocking mode of  $\text{Si}-\text{CH}_3$ .<sup>10,18</sup> However, a peak at  $879\text{ cm}^{-1}$  is observed to increase, and, because this is also usually associated with  $\text{Si}-\text{C}$  bonding, its increase is counterintuitive, although this has also been observed by Pryce-Lewis et al.<sup>10</sup> An alternative assignment for this peak is  $\text{Si}-\text{H}$ ,<sup>21</sup> since this structural element is known to be present in the coating by the peak at  $\sim 2200\text{ cm}^{-1}$ , and both peaks increase slightly when the feed gas ratio is decreased. The emergence of a peak in the low ratio coating at  $\sim 930\text{ cm}^{-1}$  is most likely associated with an increasing content of  $\text{Si}-\text{OH}$  (as seen at  $3400\text{ cm}^{-1}$ ). The region at  $\sim 1100\text{ cm}^{-1}$  can contain vibrational modes from

several bonds. Literature reports refer to  $\text{Si}-\text{CH}_2-\text{Si}$  wagging modes at  $\sim 1090-1020\text{ cm}^{-1}$ , as well as  $\text{Si}-\text{O}-\text{C}$  across a similar region, and  $\text{Si}-\text{CH}$  at  $980\text{ cm}^{-1}$  (ref 42) and from  $1150$  to  $1050\text{ cm}^{-1}$  are vibrational stretching modes of  $\text{Si}-\text{O}-\text{Si}$ .<sup>19,43</sup> It has also been reported that a broadening or doublet formation around this position is linked to longer  $\text{Si}-\text{O}$  chains.<sup>18,44</sup> Alternatively, Nowling et al.<sup>45</sup> discuss the potential for it to be related to porosity; however, this appears as more of a shoulder on the high-frequency side, rather than as a discrete peak, and thus is not considered in our interpretation. Considering all the observed vibrational modes, the interpretation of bonds in this region is difficult, unless coupled with complementary data, such as NMR. By considering the NMR data shown in Figures 2 and 3, however, a decreasing feed gas ratio is seen to lead to a coating with a high number of  $\text{Si}-\text{O}-\text{Si}$  bonds. Therefore, it is most likely that the broad peak observed in the  $1100\text{ cm}^{-1}$  region is due to this type of bonding. For a decreasing feed gas ratio, the broadening of this bond relates to an increase in the occurrence of bridging to form  $\text{Si}-\text{O}-\text{Si}$  bonds. That is, as the ratio is decreased, the coatings are developing an extended  $\text{Si}-\text{O}-\text{Si}$  network.

**B. Post-Plasma Reactions.** 1.  $^{13}\text{C}$  CP/MAS NMR.  $^{13}\text{C}$  CP/MAS NMR spectra for the coatings produced at feed gas ratios of 0.3, 0.18, and 0.05 display only three significant peaks, two of which (at  $-3$  and  $+1\text{ ppm}$ ) can be attributed to the presence of methyl groups and the third (a very small peak at  $+50\text{ ppm}$ ) can be assigned to  $-\text{O}-\text{CH}_2-$ .<sup>46</sup> This relatively simple spectrum indicates that the formation of new bonds at C-centered radicals, produced by C-H bond fissions, is not a major contributor to the plasma polymer formation. Instead, it appears that the monomer fragments cross-link mainly via the formation of new  $\text{Si}-\text{O}$  bonds and, hence, a major reaction pathway is removal of methyl groups from the monomer.<sup>47</sup> The decreased C/Si ratio is consistent with this postulate of cleavage of methyl groups from the monomer during plasma activation. Upon storage of the coatings in air over a period of 8 weeks, there was only a very small shift in the peak heights in  $^{13}\text{C}$  CP/MAS NMR spectra, indicating that no substantial changes occurred post-plasma in the carbon bonding. Thus, any observed shifts in SPE  $^{29}\text{Si}$  MAS and  $^{29}\text{Si}$  CP/MAS NMR spectra with time are most likely to involve  $\text{Si}-\text{O}$  or  $\text{Si}-\text{H}$  bonds, rather than additional changes to the extent of methyl substitution. This finding allows better interpretation of the  $^{29}\text{Si}$  NMR data, since there are regions in the spectra where overlaps of resonances exist, and resonance lines may be assigned to bonding of either  $\text{Si}-\text{O}$ ,  $\text{Si}-\text{H}$ , or  $\text{Si}-\text{Me}$  (Figure 5). If a change in intensities occurs in one of these resonance lines, it must involve  $\text{Si}-\text{O}$  or  $\text{Si}-\text{H}$  bonding.

2. *The 0.3 TMDSO-to- $\text{O}_2$  Ratio Coating.* Changes in intensities of resonance lines in  $^{29}\text{Si}$  CP/MAS NMR spectra during post-plasma storage (Figure 7) were followed over a period of eight weeks. It was observed that there are changes in intensities for almost all  $^{29}\text{Si}$  resonance lines. For the coating with a TMDSO-to-oxygen ratio of 0.3 (Figure 7a),  $^{29}\text{Si}$  NMR resonance lines at  $-15\text{ ppm}$  and  $-62\text{ ppm}$  increase in intensity; they are assigned to  $\text{M}^{\text{OH}}$  and  $\text{D}^{\text{OH}}$ , respectively. The intensity of the resonance line at  $-106\text{ ppm}$  also increases, corresponding to Q-type bonding. The resonance line at  $-97\text{ ppm}$  ( $\text{T}^{\text{OH}}$ ) remains constant. Resonances at  $-32\text{ ppm}$  and  $-49\text{ ppm}$  correspond to hydrogen-substituted bonds, and their intensities decrease over time. The intensities of the resonances corresponding to multiple substitutions by OH at  $-43\text{ ppm}$  and  $-89\text{ ppm}$ , which are assigned to  $\text{M}^{(\text{OH})_2}$  and  $\text{D}^{(\text{OH})_2}$ ,

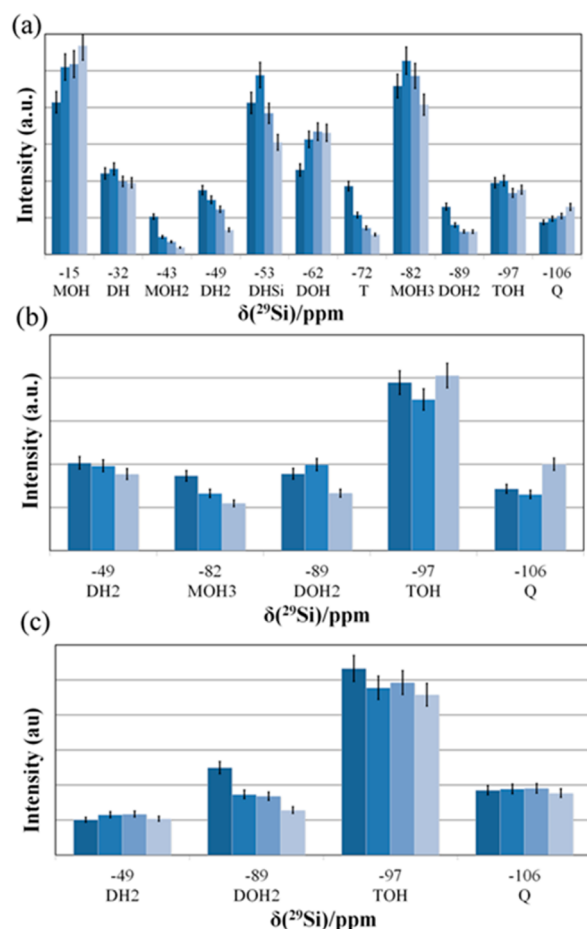


**Figure 7.** Changes in intensities of resonance lines in  $^{29}\text{Si}$  CP/MAS NMR spectra over eight weeks for TMDSO-to- $\text{O}_2$  ratio coatings of (a) 0.3, (b) 0.18, and (c) 0.05. For panels (a) and (c), measurements were taken after storage periods of 24 h, and at 1, 3, and 8 weeks. For panel (b), measurements were taken at 24 h, and at 2 and 8 weeks. Only significant peaks and those that showed clear changes have been plotted. Error bars were determined from previous measurements and from the peak height identification procedure.

respectively, also decrease. Of note are resonance lines at  $-53$  ppm and  $-82$  ppm (assigned to  $\text{D}^{\text{HSi}}$  and  $\text{M}^{\text{(OH)}_3}$ , respectively); the intensities of these are observed to initially increase but then decrease, becoming substantially lower at the end of the eight-week period. The general trend was for the intensity of the resonances with hydrogenated functionality and multi-ply substituted hydroxylated functionality to decrease over time. It is suggested that some of the multi-ply substituted groups are decreasing and form a cross-linked O–Si–O structure. In contrast, the singly substituted hydroxylated functionality increased. The increase in this intensity is most likely due to the hydroxylation of the singly substituted hydrogenated functionality. However, since the resonance intensities are not quantitative, because of the unequal absorption cross-sections, care must be exercised in interpretation when comparing peak heights of resonance lines.

**3. The 0.18 TMDSO-to- $\text{O}_2$  Ratio Coating.** Figure 7b shows the changes in  $^{29}\text{Si}$  CP/MAS NMR spectra due to post-plasma reactions for the coating with a TMDSO-to-oxygen ratio of 0.18. There is a significant reduction in the number of resonance lines and, therefore, the types of bonds deposited under TMDSO-to-oxygen ratio of 0.18, compared to the

coatings deposited under a TMDSO-to-oxygen ratio of 0.3. However, for the resonances observed, there were similar post-plasma changes when comparing the intensities between the 0.3 ratio coatings and the 0.18 ratio coatings. Specifically, a decrease in the intensity of the  $^{29}\text{Si}$  NMR resonance lines assigned to multi-ply substituted hydrogenated Si and some of the hydroxylated bonds, as shown by a decrease in the intensity of the resonances at  $-49$  ppm  $\text{D}^{\text{(H)}_2}$ ,  $-82$  ppm  $\text{M}^{\text{(OH)}_3}$ , and  $-89$  ppm  $\text{D}^{\text{(OH)}_2}$ . The intensity of the resonance line at  $-97$  ppm ( $\text{T}^{\text{OH}}$ ) remained constant and by the eight-week mark, the intensity of the resonance line at  $-106$  ppm ( $\text{Q}^{\text{(4)}}$ ) had significantly increased. This is indicative of the further development of a O–Si–O cross-linked structure.

**4. The 0.05 TMDSO-to- $\text{O}_2$  Ratio Coating.** Figure 7c shows the changes in intensities of resonance lines in  $^{29}\text{Si}$  CP/MAS NMR spectra for the coating with a TMDSO-to-oxygen ratio of 0.05, which is a highly inorganic and cross-linked coating with a pronounced change in Si–O bonding, compared to the 0.3 ratio coatings and the 0.18 ratio coatings.

There are broad but small resonances in the  $-10$  ppm to  $-20$  ppm (M) region and in the  $-50$  ppm to  $-60$  ppm (D) region, which do not change with time. The intensity of a shoulder resonance line at  $-89$  ppm ( $\text{D}^{\text{(OH)}_2}$ ) decreases while the intensity of another shoulder resonance at  $-106$  ppm ( $\text{Q}^{\text{(4)}}$ ) remains constant. Intensities of these resonance lines showed only minor changes during post-plasma reactions. Thus, it appears that this coating is quite stable toward post-plasma chemical changes upon storage in air, similar to a HMDSO plasma polymer previously reported to show only small changes upon storage.<sup>19</sup>

## IV. DISCUSSION

**A. Structure of Plasma-Polymerized Organosilicone Coatings.** The results presented above from the quantitative SPE  $^{29}\text{Si}$  MAS NMR studies on coatings deposited with TMDSO-to-oxygen ratios of 0.5, 0.375, and 0.3 describe a cross-linked siloxane structure. A high proportion of the Si atoms are bonded with four O atoms, and there is only a small percentage of Si that have Si–R terminations, where R is most likely  $\text{CH}_3$ , OH, or H. When the TMDSO-to-oxygen ratio is decreased, there is an increase toward T- and Q-type bonding structures.

Assink et al.<sup>48</sup> previously presented semiquantitative data on rf PECVD of HMDSO. The deposition systems used in that study and others<sup>30,31,39</sup> do not modify the starting monomer to the same degree as is reported in this study, probably because of a combination of plasma power and frequency. Assink et al. post-plasma heat-treated the coatings, and this then modified the coating chemistry and structure in a more inorganic direction, toward that achieved in this study under low TMDSO-to-oxygen ratio conditions without the need for post-plasma treatment. While it is reported that PECVD produces highly cross-linked structures, as shown, for example, by Wu and Gleason<sup>30</sup> reporting that 10% of the Si are in Q-type configurations, the data presented here describe one coating, which displays a higher degree of cross-linking, where 55% of the Si–O are in Q-type configurations. The cross-linking efficiency of our deposition process is due to the relatively high power and the high frequency of the plasma, as well as the reactor geometry, which was optimized by trialing various arrangements of gas feed “showerheads” and microwave (mw) antennae. The microwave plasma fragments the monomer molecules through reactions with excited oxygen, free radicals,

molecular fragments, electrons, ions, and photons. As described in this study, there is a large influence of the TMDSO-to-oxygen ratio on the degree of cross-linking. It is apparent that the oxygen plays a major role in the fragmentation process of the TMDSO molecules and in the subsequent formation of the coating; this was also reported by Lin and Chen,<sup>49</sup> Wu and Gleason,<sup>30</sup> Hegemann et al.,<sup>50</sup> and Korzec et al.<sup>51</sup>

**B. Post-Plasma Reactions.** Coatings produced for the study of post-plasma reactions displayed considerable variation in siloxane structural bonding. The coatings deposited were drastically altered from their parent monomer. At a high TMDSO-to-oxygen ratio, the deposited coatings were organic in nature, whereas coatings produced at lower ratios were found to change to an inorganic “glass-like” composition.

High ratio coatings have been found to adhere well to both PMMA and PC.<sup>16</sup> On the other hand, low ratio coatings, because of their highly cross-linked nature, have better barrier properties and are scratch-resistant. This control of coating chemistry has been used to make adherent durable protective coatings on polycarbonate.<sup>16,52</sup>

The high ratio coating (TMDSO-to-O<sub>2</sub> ratio of 0.3) underwent post-plasma reactions that involved a reduction in the organic nature of the coating. In Figure 7a, there is an evident reduction in the intensity of the resonance lines corresponding to hydrogenated and some hydroxylated bond configurations, D<sup>H</sup>, D<sup>H<sub>2</sub></sup>, D<sup>H<sub>Si</sub></sup>, M<sup>(OH)<sub>3</sub></sup>, M<sup>(OH)<sub>2</sub></sup>, and D<sup>(OH)<sub>2</sub></sup>. An increase in the intensities of the resonance lines assigned to Q-type bonding, which signifies an increase in the cross-linked O–Si–O structures. The quantitative NMR data show that the coating deposited under a TMDSO-to-oxygen ratio of 0.3 is comprised of ~55% of this type of structure. When a small increase in the resonance lines in this region is observed, then this is expected to correspond to a relatively large change in coating properties, because of the dominance of Q-type Si structures. This concept will be explored in further research. The development of a cross-linked O–Si–O network was also observed as an increase in the Si–O–Si vibrational mode in the FTIR spectra. The FTIR analysis also showed a decrease in the –OH signal, which can be linked to the decrease in the multiply substituted hydroxylated bond configurations. It is suggested that some of the Si atoms that are multiply-substituted with –OH lose one or two of these substituents and form the cross-linked O–Si–O structure. Potentially, hydrogenated configurations may also become hydroxylated, adding to the M<sup>OH</sup> and D<sup>OH</sup> bond types. Mabboux and Gleason<sup>33</sup> have also noted the unstable nature of the Si–H bond in such polymers and its tendency to be hydrolyzed to Si–OH and then undergo further reactions to form the O–Si–O cross-linked structure.

Of interest is the apparent stability of the Si-CH<sub>3</sub> structural units, as identified in the FT-IR spectra and also in the <sup>13</sup>C CP/MAS NMR. While, during plasma deposition, the Si–C bond is cleaved (by methyl abstraction), once incorporated into the coating, it does not appear to undergo post-plasma reactions.

There is similar behavior for the coating with a TMDSO-to-oxygen ratio of 0.18; however, at this ratio, the post-plasma reactions are reduced, relative to coatings with a TMDSO-to-oxygen ratio of 0.3. For the coating with a TMDSO-to-oxygen ratio of 0.05, the chemical structure is simplified and the reactive groups seen in the coatings produced at higher ratios are not present. The structure is largely composed of T- and Q-type bond configurations. The post-plasma reactions showed only slight changes; thus, the low ratio coating is relatively

stable under ambient air storage conditions when compared to coatings made using the other two TMDSO-to-oxygen ratios.

It is hypothesized that the relatively lesser chemical stability of the high ratio coating is the cause for the crazing observed in the graded coatings. As it undergoes post-plasma reactions, it develops more of a cross-linked network and becomes less compliant. The high-ratio coating was intended to provide a compliant layer to match mechanically with the soft plastic substrates. Changes with time in this region will affect the stress balance within the coating and may lead to the stress crazing that we have observed.

Chemically stable coatings have been identified as those produced with a high amount of added oxygen (that is, a low TMDSO-to-oxygen ratio). However, while stable coatings can be achieved via this manner, it results in a coating that is not mechanically compatible with the underlying substrate. The highly cross-linked nature of the low-ratio coating leads to a hardness that is mechanically mismatched with plastic substrates and, consequently, this hard coating has been found not to adhere well to plastic substrates, such as PMMA<sup>53</sup> and polycarbonate.<sup>12,52</sup> Further work is underway to correlate the surface chemistry to the TMDSO-to-oxygen ratio via XPS analysis and to characterize the effects of post-plasma reactions on the chemical and mechanical properties, such as stress, hardness, thickness, and coating mass.<sup>54</sup> In addition, investigations are underway to identify an approach that results in both mechanical compliance and chemical stability. Alternative monomers (such as HMDSO) might be advantageous for the lesser oxidation of their plasma polymers, as reported by Gengenbach et al.<sup>19</sup> and Haque et al.;<sup>55</sup> however, their lower deposition rate may limit their suitability when thicker protective coatings are required. This work is relevant to the ongoing development of abrasion-resistant hardcoating for use on plastics in applications such as ophthalmic lenses and automotive components, and in the aerospace industry.

## V. CONCLUSIONS

Quantitative SPE <sup>29</sup>Si MAS NMR data were collected on three coatings of varying TMDSO-to-oxygen ratios. By combining FTIR data, SPE <sup>29</sup>Si MAS NMR, <sup>29</sup>Si CP/MAS, and <sup>13</sup>C CP/MAS NMR data, a complete picture of the bonding environments in coatings was elucidated.

The microwave plasma was seen to drastically change the parent monomer molecular structure and result in a high level of molecular fragmentation. This resulted in coatings that consisted predominantly of T- and Q-type siloxane bonding, which corresponds to a high level of cross-linking, higher than for similar coatings previously reported.

The post-plasma reactions were studied for three coatings of different TMDSO-to-oxygen ratios over a period of eight weeks. High-ratio coatings exhibited the most varied chemistry and, subsequently, the most extensive post-plasma reactions. Unstable hydrogenated functionalities were found to undergo reactions to singly hydroxylated Si–OH groups. Multiply substituted hydroxylated groups underwent cross-linking via the conversion of some of the Si–OH bonding structure to a O–Si–O structure. It was found that coatings produced with a low TMDSO-to-O<sub>2</sub> ratio had reduced retention of organic chemical functionality and, hence, underwent less-extensive post-plasma reactions, leading to a more stable coating on storage in air. However, the mismatch in mechanical properties of the hard low-ratio coating with PC and PMMA substrates poses some problems, necessitating the use of a graded coating



to avoid interfacial stress. Work is currently underway on linking the chemical changes to observed physical changes in coatings, such as hardness, modulus, stress, and mass. Future work toward identifying a stable compliant intermediate layer is also required.

## AUTHOR INFORMATION

### Corresponding Author

\*Tel.: +61 8 8302 3833. Fax: +61 8 8302 5639. E-mail: colin.hall@unisa.edu.au.

### Author Contributions

The manuscript was written through contributions of all authors. All authors have given approval to the final version of the manuscript.

### Notes

The authors declare no competing financial interest.

## ACKNOWLEDGMENTS

The authors acknowledge the contributions of Kamil Zuber and Maria Patterson, for assistance with FT-IR measurements and sample preparation. Financial support was received from the Australian Federal Government through the Cooperative Research Centre for Advanced Automotive Technology (AutoCRC). O.N.A. and M.L. acknowledge STINT (Sweden) for funding of the scientific collaboration and research visits to IWRI at the University of South Australia. The Foundation in Memory of J.C. and Seth M. Kempe are gratefully acknowledged for grants, from which NMR spectrometer at LTU has been upgraded.

## REFERENCES

- (1) Tashiro, H.; Nakaya, M.; Hotta, A. Enhancement of the Gas Barrier Property of Polymers by DLC Coating with Organosilane Interlayer. *Diamond Rel. Mater.* **2013**, *35*, 7–13.
- (2) Plog, S.; Schneider, J.; Walker, M.; Schulz, A.; Stroth, U. Investigations of Plasma Polymerized SiO<sub>x</sub> Barrier Films for Polymer Food Packaging. *Surf. Coat. Technol.* **2011**, *205*, S165–S170.
- (3) Noborisaka, M.; Kodama, H.; Nagashima, S.; Shirakura, A.; Horiuchi, T.; Suzuki, T. Synthesis of Transparent and Hard SiOC(–H) Thin Films on Polycarbonate Substrates by PECVD Method. *Surf. Coat. Technol.* **2012**, *206*, 2581–2584.
- (4) Seubert, C.; Nietering, K.; Nichols, M.; Wykoff, R.; Bollin, S. An Overview of the Scratch Resistance of Automotive Coatings: Exterior Clearcoats and Polycarbonate Hardcoats. *Coatings* **2012**, *2*, 221–234.
- (5) Wrobel, A. M. Aging Process in Plasma-Polymerized Organosilicon Thin Films. *J. Macromol. Sci., Chem.* **1985**, *22*, 1089–1100.
- (6) Bieg, K. W.; Wischmann, K. B. Plasma-Polymerized Organosilanes as Protective Coatings for Solar Front-Surface Mirrors. *Sol. Energy Mater.* **1980**, *3*, 301–316.
- (7) Kryszewski, M.; Wrobel, A. M.; Tyczkowski, J. Plasma-Polymerized Organosilicon Thin Films Structure and Properties. In *Plasma Polymerization*; American Chemical Society: Washington, DC, 1979; Vol. 108, pp 219–236.
- (8) Hegemann, D.; Brunner, H.; Oehr, C. Evaluation of Deposition Conditions to Design Plasma Coatings Like SiO<sub>x</sub> and a-C:H on Polymers. *Surf. Coat. Technol.* **2003**, *174–175*, 253–260.
- (9) Hegemann, D.; Oehr, C.; Fischer, A. Design of Functional Coatings. *J. Vac. Sci. Technol., A* **2004**, *23*, 5–11.
- (10) Pryce Lewis, H. G.; Edell, D. J.; Gleason, K. K. Pulsed-PECVD Films from Hexamethylcyclotrisiloxane for Use as Insulating Biomaterials. *Chem. Mater.* **2000**, *12*, 3488–3494.
- (11) Coclite, A. M.; De Luca, F.; Gleason, K. K. Mechanically Robust Silica-Like Coatings Deposited by Microwave Plasmas for Barrier Applications. *J. Vac. Sci. Technol., A* **2012**, *30*, 061502:061501–061509.
- (12) Cui, L.; Ranade, A. N.; Matos, M. A.; Pingree, L. S.; Frot, T. J.; Dubois, G.; Dauskardt, R. H. Atmospheric Plasma Deposited Dense Silica Coatings on Plastics. *ACS Appl. Mater. Interfaces* **2012**, *4*, 6587–6598.
- (13) Bahroun, K.; Behm, H.; Mitschker, F.; Awakowicz, P.; Dahlmann, R.; Hopmann, C. Influence of Layer Type and Order on Barrier Properties of Multilayer PECVD Barrier Coatings. *J. Phys. D: Appl. Phys.* **2014**, *47*, 015201.
- (14) Beckmann, R.; Nauenburg, K. D.; Naumann, T.; Patz, U.; Ickes, G.; Hagedorn, H.; Snyder, J. A New High-Rate Deposition Process for Scratch- and Wipe-Resistant Coatings for Optical and Decorative Plastic Parts. In *Proceedings of the 44th Annual Technical Conference of SVC*, Philadelphia, PA, April 21–26, 2001.
- (15) Huang, C.; Yu, Q. Deposition of Silicon Oxide Hard Coatings by Low-Temperature Radio-Frequency Plasmas. *J. Appl. Polym. Sci.* **2010**, *116*, 245–251.
- (16) Griesser, H.; Murphy, P.; Hall, C. Craze Resistant Plastic Article and Method of Production. U.S. Patent 20080096014 A1, April 24, 2008.
- (17) Hall, C. J.; Murphy, P. J.; Griesser, H. J. Direct Imaging of Mechanically and Chemically Graded Organosilicone Microwave PECVD Coatings. *ACS Appl. Mater. Interfaces* **2014**, *6*, 1279–1287.
- (18) Rau, C.; Kulisch, W. Mechanisms of Plasma Polymerization of Various Silico-Organic Monomers. *Thin Solid Films* **1994**, *249*, 28–37.
- (19) Gengenbach, T. R.; Griesser, H. J. Post-Deposition Ageing Reactions Differ Markedly between Plasma Polymers Deposited from Siloxane and Silazane Monomers. *Polymer* **1999**, *40*, 5079–5094.
- (20) Hegemann, D.; Brunner, H.; Oehr, C. Plasma Treatment of Polymers to Generate Stable, Hydrophobic Surfaces. *Plasmas Polym.* **2001**, *6*, 221–235.
- (21) Benissad, N.; Boisse-Laporte, C.; Vallée, C.; Granier, A.; Goulet, A. Silicon Dioxide Deposition in a Microwave Plasma Reactor. *Surf. Coat. Technol.* **1999**, *116–119*, 868–873.
- (22) Gengenbach, T. R.; Chatelier, R. C.; Griesser, H. J. Characterization of the Ageing of Plasma-Deposited Polymer Films: Global Analysis of X-Ray Photoelectron Spectroscopy Data. *Surf. Interface Anal.* **1996**, *24*, 271–281.
- (23) Wrobel, A. M.; Kowalski, J.; Grebowicz, J.; Kryszewski, M. Thermal Decomposition of Plasma-Polymerized Organosilicon Thin Films. *J. Macromol. Sci., Chem.* **1982**, *17*, 433–452.
- (24) Muir, B. W.; Thissen, H.; Simon, G. P.; Murphy, P. J.; Griesser, H. J. Factors Affecting the Adhesion of Microwave Plasma Deposited Siloxane Films on Polycarbonate. *Thin Solid Films* **2006**, *500*, 34–40.
- (25) Wertheimer, M. R.; Klemberg-Sapieha, J. E.; Schreiber, H. P. Advances in Basic and Applied Aspects of Microwave Plasma Polymerization. *Thin Solid Films* **1984**, *115*, 109–124.
- (26) Goujon, M.; Belmonte, T.; Henrion, G. OES and FTIR Diagnostics of HMDSO/O<sub>2</sub> Gas Mixtures for SiO<sub>x</sub> Deposition Assisted by RF Plasma. *Surf. Coat. Technol.* **2004**, *188–189*, 756–761.
- (27) Bapin, E.; von Rohr, P. R. Deposition of SiO<sub>2</sub> Films from Different Organosilicon/O<sub>2</sub> Plasmas under Continuous Wave and Pulsed Modes. *Surf. Coat. Technol.* **2001**, *142–144*, 649–654.
- (28) Shah, F. U.; Glavatskih, S.; Höglund, E.; Lindberg, M.; Antzutkin, O. N. Interfacial Antiwear and Physicochemical Properties of Alkylborate-Dithiophosphates. *ACS Appl. Mater. Interfaces* **2011**, *3*, 956–968.
- (29) Bertermann, R.; Kröger, N.; Tacke, R. Solid-State <sup>29</sup>Si MAS NMR Studies of Diatoms: Structural Characterization of Biosilica Deposits. *Anal. Bioanal. Chem.* **2003**, *375*, 630–634.
- (30) Wu, Q.; Gleason, K. K. Plasma-Enhanced CVD of Organosilicate Glass (OSG) Films Deposited from Octamethyltrisiloxane, Bis(Trimethylsiloxy)Methylsilane, and 1,1,3,3-Tetramethyldisiloxane. *Plasmas Polym.* **2003**, *8*, 31–41.
- (31) Wang, Y.; Zhang, J.; Shen, X. Surface Structures Tailoring of Hexamethyldisiloxane Films by Pulse RF Plasma Polymerization. *Mater. Chem. Phys.* **2006**, *96*, 498–505.
- (32) Roualdes, S.; Berjoan, R.; Durand, J. <sup>29</sup>Si NMR and Si 2p XPS Correlation in Polysiloxane Membranes Prepared by Plasma Enhanced Chemical Vapor Deposition. *Sep. Purif. Technol.* **2001**, *25*, 391–397.

- (33) Mabboux, P.-Y.; Gleason, K. K. Chemical Bonding Structure of Low Dielectric Constant Si:O:C:H Films Characterized by Solid-State NMR. *J. Electrochem. Soc.* **2005**, *152*, F7–F13.
- (34) Eckert, H. Structural Concepts for Disordered Inorganic Solids. Modern NMR Approaches and Strategies. Invited Review. *Ber. Bunsen. Phys. Chem.* **1990**, *94*, 1062–1085.
- (35) Liehr, M., Device for Producing Plasma, U.S. Patent 6,194,835, May 27, 2001.
- (36) Eberhard, R.; Muegge, H.; Konstatin, R., Device for Generating Plasma in Vacuum Container, DE Patent 19628954, Jan. 22, 1998.
- (37) Marsmann, H. C.; Uhlig, F. Silicon-29 NMR Data of C<sub>4</sub>H<sub>14</sub>OSi<sub>2</sub>. In *Landolt-Börnstein—Group III Condensed Matter, Chemical Shifts and Coupling Constants for Silicon-29*; Gupta, R. R.; Lechner, M. D., Eds.; Springer-Verlag: Berlin, Heidelberg, 2008; Vol. 35F, p 315.
- (38) Alexander, M. R.; Jones, F.; Short, R. D. Radio-Frequency Hexamethyldisiloxane Plasma Deposition: A Comparison of Plasma and Deposit- Chemistry. *Plasmas Polym.* **1997**, *2*, 277–300.
- (39) Tajima, I.; Yamamoto, M. Spectroscopic Study on Chemical Structure of Plasma-Polymerized Hexamethyldisiloxane. *J. Polym. Sci., Part A: Polym. Chem.* **1985**, *23*, 615–622.
- (40) Levy, G. C. Vol. 4, *Topics in Carbon-13 NMR Spectroscopy*; Wiley-Interscience, New York, 1980; p 304.
- (41) Mei-Li, Z.; Ya-Bo, F.; Qiang, C.; Yuan-Jing, G. Deposition of SiO<sub>x</sub> Barrier Films by O<sub>2</sub>/TMDSO RF-PECVD. *Chin. Phys.* **2007**, *16*, 1101–1104.
- (42) Jousseume, V.; Rochat, N.; Favennec, L.; Renault, O.; Passemard, G. Mechanical Stress in PECVD a-SiC:H: Aging and Plasma Treatments Effects. *Mater. Sci. Semicond. Process.* **2004**, *7*, 301–305.
- (43) Kamitsos, E. I.; Patsis, A. P.; Kordas, G. Infrared-Reflectance Spectra of Heat-Treated Sol-Gel-Derived Silica. *Phys. Rev. B* **1993**, *48*, 12499.
- (44) Wright, N.; Hunter, M. J. Organosilicon Polymers. III. Infrared Spectra of the Methylpolysiloxanes. *J. Am. Chem. Soc.* **1947**, *69*, 803–809.
- (45) Nowling, G. R.; Yajima, M.; Babayan, S. E.; Moravej, M.; Yang, X.; Hoffman, W.; Hicks, R. F. Chamberless Plasma Deposition of Glass Coatings on Plastic. *Plasma Sources Sci. Technol.* **2005**, *14*, 477.
- (46) Rodríguez-Baeza, M.; Zapata, M.; Valeria, I.; Yoshida, P. Synthesis and Structure of Crosslinked Poly[(Methylsiloxane)-Co-(Oxymethylene)] Copolymers. *Macromol. Rapid Commun.* **1997**, *18*, 747–754.
- (47) Coopes, I. H.; Griesser, H. J. The Structure of Organosilicon Plasma-Polymerized Coatings on Metal Substrates. *J. Appl. Polym. Sci.* **1989**, *37*, 3413–3422.
- (48) Assink, R. A.; Hays, A. K.; Bild, R. W.; Hawkins, B. L. <sup>29</sup>Si Nuclear Magnetic Resonance Study of Plasma-Polymerized Hexamethyldisiloxane. *J. Vac. Sci. Technol., A* **1985**, *3*, 2629–2633.
- (49) Lin, Y. S.; Chen, C. L. Wear Resistance of Low-Temperature Plasma-Polymerized Organosilica Deposited on Poly(Ethylene Terephthalate): The Effect of O<sub>2</sub> Addition. *Plasma Process. Polym.* **2006**, *3*, 650–660.
- (50) Hegemann, D.; Vohrer, U.; Oehr, C.; Riedel, R. Deposition of SiO<sub>x</sub> Films from O<sub>2</sub>/HMDSO Plasmas. *Surf. Coat. Technol.* **1999**, *116–119*, 1033–1036.
- (51) Korzec, D.; Traub, K.; Werner, F.; Engemann, J. Remote Deposition of Scratch Resistant Films by Use of Slot Antenna Microwave Plasma Source. *Thin Solid Films* **1996**, *281–282*, 143–145.
- (52) Hall, C. J.; Murphy, P. J.; Griesser, H. J. Etching and Deposition Mechanism of an Alcohol Plasma on Polycarbonate and Poly-(Methylmethacrylate): An Adhesion Promotion Mechanism for Plasma Deposited a-SiO<sub>x</sub>C<sub>y</sub>H<sub>z</sub> Coating. *Plasma Process. Polym.* **2012**, *9*, 855–865.
- (53) Hall, C. J.; Murphy, P. J.; Griesser, H. J. Hydroxyl Radical Etching Improves Adhesion of Plasma-Deposited a-SiO<sub>x</sub>C<sub>y</sub>H<sub>z</sub> Films on Poly(Methylmethacrylate). *Plasma Process. Polym.* **2012**, *9*, 398–405.
- (54) Hall, C. J.; Murphy, P. J.; Griesser, H. J. Influence of Tetramethyldisiloxane-Oxygen Mixtures on Microwave PECVD Coating's Physical Properties and Subsequent Post Plasma Reactions, Manuscript submitted for publication, 2014.
- (55) Haque, M. S.; Naseem, H. A.; Brown, W. D. Post-Deposition Processing of Low Temperature PECVD Silicon Dioxide Films for Enhanced Stress Stability. *Thin Solid Films* **1997**, *308–309*, 68–73.